Oceanologia, corrected, in press
Polish Academy of Sciences
Institute of Oceanology
Open access article under the CC BY license
https://doi.org/10.5697/TDRI2173

Estimating net fixed nitrogen loss in the Baltic Sea from deep-water excess N_2 accumulation

Beata Szymczycha[1,*], Magdalena Diak[1], Marc J. Silberberger[2]

Abstract

We quantified excess N_2 accumulation below the halocline of the Baltic Proper using *in situ* N_2/Ar measurements combined with N_2/Ar estimates derived from the three-dimensional ERGOM–MOM biogeochemical model. The observed temporal increase in excess N_2 was subsequently converted to nitrogen loss. The analysis focused on the post-2014 Major Baltic Inflow period, when deep-water ventilation effects had largely subsided and stratification with progressive oxygen depletion was re-established. Both observations and model simulations showed increasing excess N_2 below the halocline, particularly in the Eastern Gotland Basin (EGB). Observation-based estimates of nitrogen loss amounted to approximately 80.8 ± 22.7 kt N yr^{-1} in the EGB, $\sim 15.6 \pm 7.8$ kt N yr^{-1} in the Bornholm Basin (BB), and $\sim 9.3 \pm 4.1$ kt N yr^{-1} in the Gdańsk Basin (GB). Model-derived estimates were consistently lower, but basin-specific comparisons revealed no significant differences between observational and temporally matched model-derived excess N_2 accumulation trends. The obtained values of net fixed nitrogen loss fall within the lower range of published Baltic Sea estimates, likely because the N_2/Ar approach reflects integrated net accumulation of dissolved N_2 rather than gross instantaneous denitrification rates. These results demonstrate that deep-water excess N_2 accumulation provides an integrative basis for estimating first-order net fixed nitrogen loss in stratified marine systems such as the Baltic Sea.

Keywords

ERGOM-MOM model; Denitrification; Gotland Deep; Excess nitrogen; N_2/Ar

[1] *Marine Chemistry and Biochemistry Department, Institute of Oceanology, Polish Academy of Sciences, Sopot, Poland*
[2] *Department of Fisheries Oceanography and Marine Ecology, National Marine Fisheries Research Institute, Gdynia, Poland*
***Correspondence**: beat.sz@iopan.gda.pl (B. Szymczycha)

Received: 17 February 2026; **revised:** 14 July 2026; **accepted**: 2 September 2026

1. Introduction

Nitrogen (N) is a fundamental element for life, required for the synthesis of nucleic acids and proteins, and often limits biological production in marine ecosystems despite the abundance of atmospheric dinitrogen gas (N_2). The marine N cycle is largely governed by microbially mediated redox reactions that transform N between oxidized and reduced forms. N_2 fixation introduces N into the system, but N_2 itself is biologically inert and requires the energetically expensive nitrogenase enzyme complex for activation, and is therefore available only to diazotrophic bacteria and archaea. In contrast, denitrification and anaerobic ammonium oxidation (anammox) convert fixed N species such as nitrate (NO_3^-), nitrite (NO_2^-), ammonium (NH_4^+) into N_2 thereby representing the dominant processes removing bioavailable N from the ocean (Codispoti et al., 2001; Capone et al., 2008; Lam and Kuypers, 2011). In oxygen-depleted or anoxic environments, NO_3^- can serve as an alternative electron acceptor for microbial respiration, resulting in the stepwise reduction of NO_3^- to N_2 through denitrification. Concurrently, anammox bacteria oxidize NH_4^+ using NO_2^- as an electron acceptor, also producing N_2.

Various analytical approaches have been developed to quantify the loss of N through denitrification and anammox in marine systems. Among the most commonly applied techniques are the acetylene blockage method, isotope tracer experiments based on ^{15}N additions and isotope-based analyses with high analytical resolution (Nielsen and Glud, 1996; Bonaglia et al., 2016). In addition, microsensor technologies provide a non-destructive and continuous means of investigating N transformations within sediments. By tracking the accumulation of nitrous oxide (N_2O), these sensors enable near real-time estimation of benthic denitrification activity (Risgaard-Petersen et al., 2003; Meyer et al., 2008). These methods typically require advanced instrumentation such as gas chromatograph coupled with an isotope ratio mass spectrometers (GC-IRMS), gas chromatograph–mass spectrometers (GC-MS), or mem-

© 2026 The Author(s). This is the Open Access article distributed under the terms of the Creative Commons Attribution Licence.

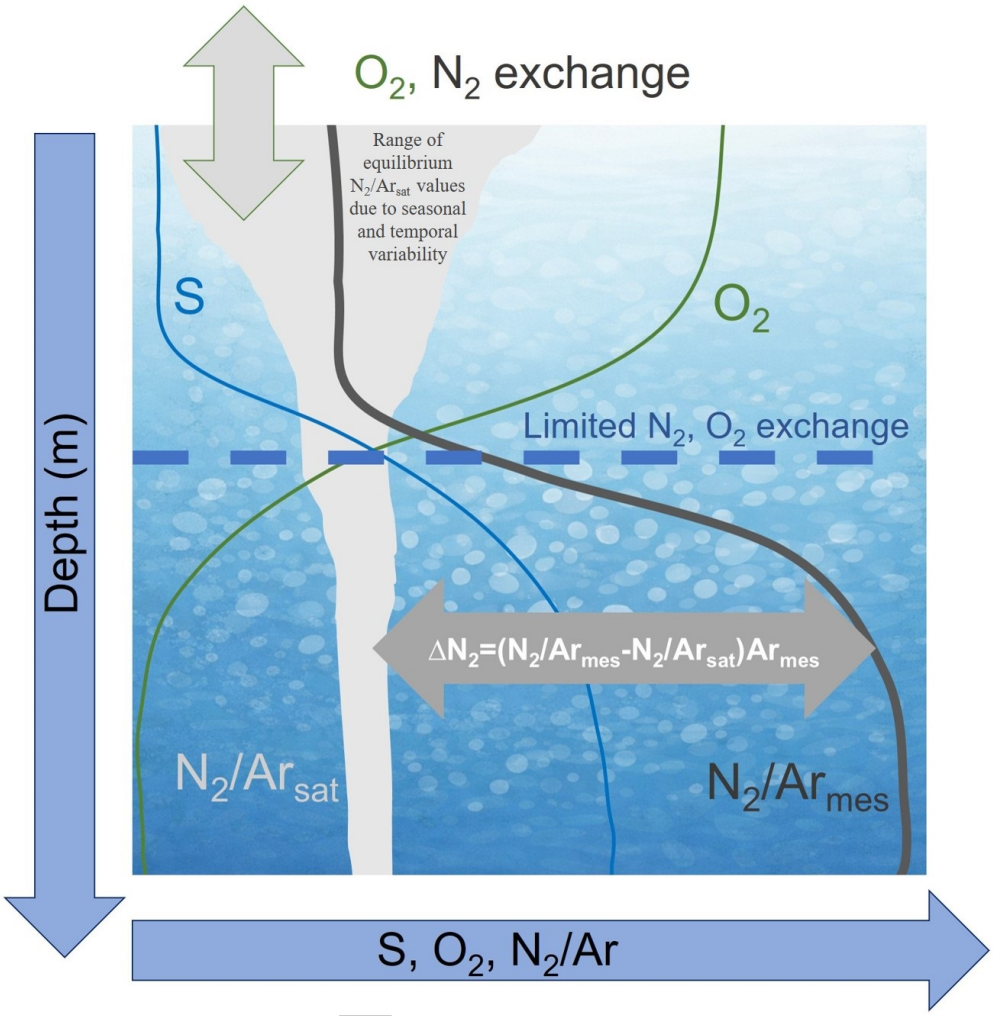


Figure 1. Conceptual schematic illustrating the principle of the N_2/Ar approach for assessing cumulative nitrogen loss in a stratified water column. A permanent halocline limits vertical mixing and air–sea gas exchange below the surface layer. Above the halocline, O_2 and N_2 are influenced by exchange with the atmosphere, whereas below the halocline gas exchange is strongly restricted. Salinity (S), dissolved oxygen (O_2), and the equilibrium N_2/Ar ratio (N_2/Ar)sat primarily reflect physical controls. Positive deviations of the measured N_2/Ar ratio (N_2/Ar mes from equilibrium indicate the accumulation of biologically produced excess dinitrogen (ΔN_2). The shaded range shown for (N_2/Ar)sat illustrates the variability in equilibrium N_2/Ar values resulting mainly from seasonal temperature changes and associated salinity variability. In contrast, the (N_2/Ar)mes profile represents observed conditions at a specific time and location and is therefore shown as a single curve. Excess ΔN_2 represents the integrated signal of deep-water ΔN_2 accumulation, occurring in oxygen-deficient deep waters.

brane inlet mass spectrometers (MIMS). Measurements performed with IRMS and GC-MS frequently involve additional preparation steps, including headspace creation or the addition of isotopically labeled standards before analysis. An alternative approach is the N_2/Ar ratio technique (Groffman et al., 2006), which provides a comparatively rapid and less labor-intensive way to assess dissolved N_2 distributions. Unlike isotope-based procedures, this method does not require extensive pre-treatment of samples and allows direct determination of dissolved N_2 concentrations in seawater. However, accurate interpretation of N_2 data requires consideration of all physical and biogeochemical processes capable of modifying N_2 concentrations within the water column. N_2 concentrations are strongly influenced by biological processes such as N_2 fixation, denitrification, and anammox, as well as by physical processes such as air–sea gas exchange, temperature-dependent solubility, bubble injection, and physical mixing (Hamme and Severinghaus, 2007). A solution to disentangle biological from physical effects is the use of inert noble gases, particularly argon (Ar), whose distribution is governed solely by physical processes. The similar solubility

properties of Ar and N_2 allow measurements of N_2/Ar ratio which is highly sensitive to denitrification signals (Devol et al., 2006; Loeffler et al., 2011; Chang et al., 2012; DeVries et al., 2012; Hamme and Emerson, 2013; Shigemitsu et al., 2016; Sivasamy et al., 2025). These signals are expressed as excess dinitrogen (ΔN_2), defined as the difference between the measured N_2/Ar ratio and the expected equilibrium N_2/Ar ratio (Hamme and Emerson, 2004, 2013; Loeffler et al., 2011; Shigemitsu et al., 2016, Sivasamy et al., 2025) (Figure 1). This approach has previously been applied in the Baltic Proper, where substantial cumulative N loss below the halocline was identified, together with pronounced spatial and seasonal variability (Sivasamy et al., 2025). In that study, the excess N_2 signal was primarily interpreted as denitrification because recent molecular investigations reported no detectable anammox-related functional genes in the deep Baltic Sea (Mazur-Marzec et al., 2024; Grabski et al., 2025), suggesting a limited contribution of anammox in these basins. However, direct denitrification rates were not quantified (Sivasamy et al., 2025). Here, we demonstrate that temporal deep-water ΔN_2 accumulation derived from N_2/Ar measurements can be used to estimate net fixed N loss in the Baltic Sea during stagnation periods owing to the unique hydrographic characteristics of this basin.

The Baltic Sea represents a strongly stratified system in which a permanent halocline restricts vertical mixing, isolating deep waters from the atmosphere and promoting the development of hypoxic and anoxic conditions (Szymczycha et al., 2019; Kuliński et al., 2022). These redox conditions favor denitrification and anammox, which are enhanced below the halocline and near the redoxcline (Hietanen and Kuparinen, 2008; Schneider et al., 2010; Loeffler et al., 2011; Dalsgaard et al., 2013; Bonaglia et al., 2016). Oxygen (O_2) conditions in the Baltic Proper are, however, impacted by Major Baltic Inflows (MBIs), during which dense, O_2-rich saline water from the North Sea enters into the deep basins (Meier, 2007; Mohrholz, 2018). These inflows temporarily ventilate deep waters, elevate O_2 concentrations, and suppress water-column N loss. During subsequent stagnation periods between inflow events, O_2 is gradually depleted by aerobic microbial respiration during organic matter (OM) mineralization, leading to the re-establishment of suboxic and anoxic conditions that intensify denitrification near the redoxcline and in deeper layers. Schneider et al. (2010) described the deep Eastern Gotland Basin during stagnation as a "biogeochemical reaction vessel" in which temporal concentration changes can be interpreted in terms of cumulative biogeochemical transformations because lateral exchange is strongly reduced and the system is affected mainly by vertical mixing. This study further demonstrated that during stagnation periods, temporal accumulation of biogeochemical tracers could be used to estimate integrated N transformation rates based on concentration changes over time. Importantly, Schneider et al. (2010) emphasized that denitrification in the Baltic deep basins is strongly coupled to the transition from oxic to anoxic conditions and the subsequent development of persistent redox stratification. Our study applies a similar conceptual framework. During the post-2014 stagnation period, vertical ventilation below the halocline was strongly reduced after the decay of the MBI signal, allowing biologically produced excess N_2 to accumulate progressively in subhalocline waters. Under these conditions, increasing ΔN_2 primarily reflects N_2 production through denitrification and anammox, while N_2 consumption through N_2 fixation and physical N_2 transport and mixing contribute to a lesser extent and remain sources of uncertainty. Therefore, under the restricted-exchange conditions prevailing during stagnation, the temporal accumulation of excess N_2 provides a first-order estimate of net fixed N loss. To evaluate this approach, we combined in situ N_2/Ar measurements collected between 2017 and 2021 (Sivasamy et al., 2025) with N_2/Ar simulations derived from the three-dimensional ERGOM–MOM ecosystem model. The model simulations were used to extend the analysis and characterize conditions over the broader period of 2016–2023. This combined observational–modeling framework provides improved constraints on net fixed N loss in the Baltic Sea and demonstrates the applicability of the N_2/Ar approach in stratified marine systems.

2. Material and methods

2.1 Study area

The study area comprised three major basins of the Baltic Proper (Figure 2; Table 1): the Eastern Gotland Basin (EGB) (stations BY15, BY15a, BY11, BY10, BY9, OM253, and Foe-B18), the Gdańsk Basin (GB) (stations P1, P1a), and the Bornholm Basin (BB) (stations IDEAL, 78M).

2.2 In situ observations and model simulations

In situ N_2/Ar measurements for these stations were obtained from Sivasamy et al. (2025) and covered the period from 2017 to 2021 (Figure 2; Table 1). Sampling focused on water layers located below the halocline and extending to approximately 5 m above the seafloor. These layers are largely isolated from direct atmospheric exchange and therefore suitable for assessing the accumulation of excess dissolved N_2 associated with N-loss processes. Temperature, salinity, and dissolved O_2 were measured in situ using a Sea-Bird SBE 911 Plus CTD system. Water samples for N_2/Ar analysis were collected from Niskin bottles into gas-tight Exetainer® vials without headspace, preserved with saturated $HgCl_2$ to inhibit biological activity, and stored at 4°C until analysis. Dissolved N_2 and Ar concentrations were determined using membrane inlet mass spectrometry (MIMS) (Sivasamy et al., 2025). The MIMS system consisted of a Pfeiffer Vacuum quadrupole mass spectrometer (model 422; QMA 400 analyzer equipped with a cross-beam ion source) coupled to a flow-through silicone cap-

In Press

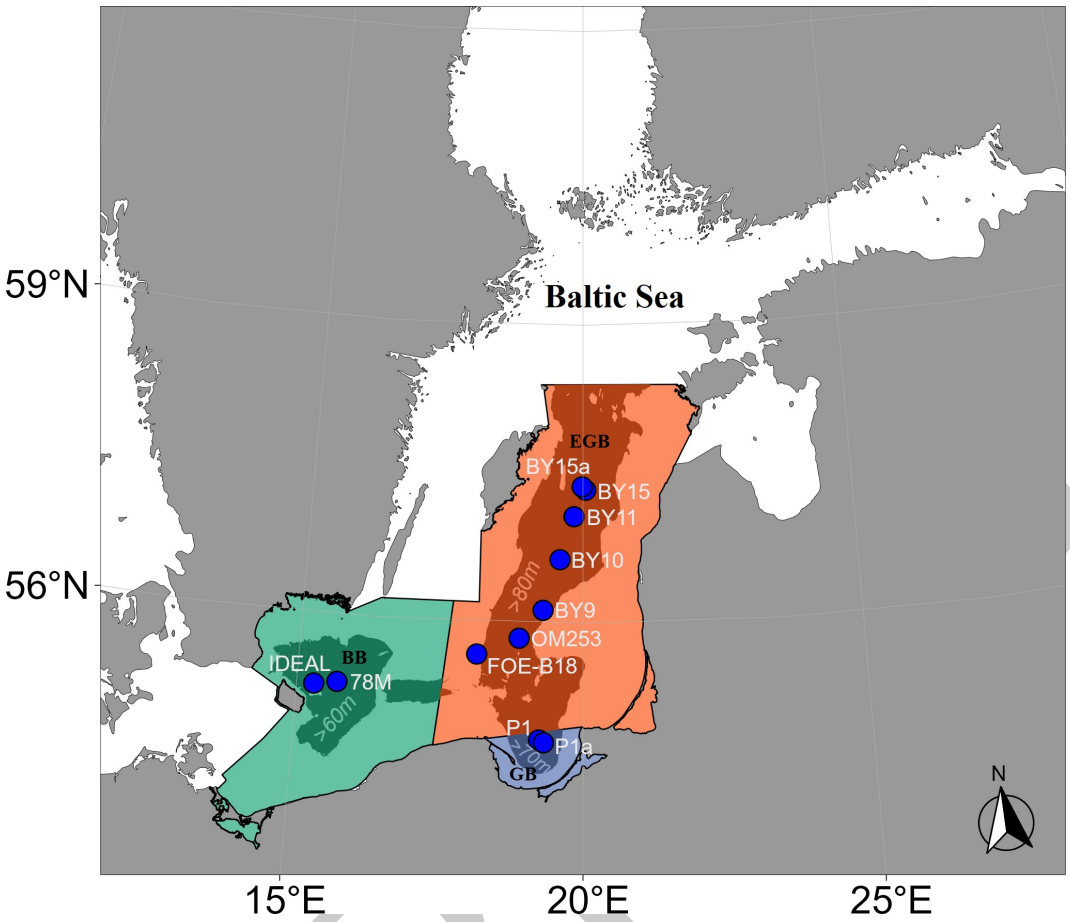


Figure 2. Map of the Baltic Proper showing the study basins and sampling stations used in this study. Colours indicate the three investigated basins: the Eastern Gotland Basin (EGB), the Bornholm Basin (BB), and the Gdańsk Basin (GB). Darker shaded areas within each basin denote regions located below the permanent halocline, which was assumed to be at 80 m in the EGB (Väli et al., 2013), 60 m in the BB (Carstensen et al., 2014), and 70 m in the GB (Paka et al., 2019). Blue circles mark the locations of in situ observation stations, including BY15, BY15a, BY11, BY10, BY9, OM253, and Foe-B18 in the EGB; IDEAL and 78M in the BB; and P1 and P1a in the GB.

illary membrane inlet (Bay Instruments, Easton, Maryland). Analytical precision was estimated to be ±0.5% for individual N_2 and Ar measurements and ±0.05% for the N_2/Ar ratio. Detection limits, defined as three times the standard deviation of five replicate measurements, were 6.5 μmol L^{-1} for N_2 and 0.015 μmol L^{-1} for Ar. Because the in situ observations were temporally limited, additional hydrographic and biogeochemical parameters were extracted for the same stations from the coupled ERGOM–MOM biogeochemical circulation model, which simulated Baltic Sea conditions for the period 2016–2023 (Neumann 2000; Neumann et al., 2022). To reduce uncertainty

Table 1. Characterization of the data representation. Number of stations and total number of samples representing each studied basin are given. EGB – Eastern Gotland Basin, BB – Bornholm Basin, GB – Gdańsk Basin; S – salinity, T – temperature, O_2 – dissolved oxygen.

Area	Method	Number of stations	Number of samples collected below halocline	Measured parameters	Calculated parameters
EGB	Measurements	7	67	N_2 /Ar_{mes}, S, T, O_2	N_2/Ar_{sat}, ΔN_2, Denitrification rate
	Model	7	18730		
BB	Measurements	2	19	N_2/Ar_{mes}, S, T, O_2	N_2/Ar_{sat}, ΔN_2, Denitrification rate
	Model	2	3135		
GB	Measurements	2	43	N_2/Ar_{mes}, S, T, O_2	N_2/Ar_{sat}, ΔN_2, Denitrification rate
	Model	2	3705		

arising from the approximation of dissolved Ar by equilibrium values in the model calculations, only data associated with modeled denitrification rates exceeding 1 nmol N L^{-1} d^{-1} were retained. This filtering restricted the analysis to conditions where biologically generated ΔN_2 signals were expected to exceed uncertainty associated with physically driven dissolved-gas variability. Denitrification rates in the model are calculated as the sum of several processes: recycling of POC (particulate organic carbon) using NO_3^-, recycling of DON (dissolved organic nitrogen) using NO_3^-, recycling of POCN (nitrogen in particulate organic carbon) using NO_3^-, recycling of DOC (dissolved organic carbon) using NO_3^-, and recycling of DOP (dissolved organic phosphorus) using NO_3^- (Neumann et al., 2022).

The model-based analysis was intentionally restricted to the period beginning in 2016 in order to minimize the influence of the MBI. In late December 2014, a large inflow of O_2-rich and saline North Sea water ventilated substantial parts of the southern and central Baltic Sea, particularly the Eastern Gotland Basin (EGB) (Gräwe et al., 2015; Mohrholz et al., 2015). Observational studies showed that the effects of this inflow persisted throughout 2015, during which oxygenated inflow waters progressively occupied the deepest layers of the EGB, including station BY15. Enhanced ventilation and intensified mixing during this period temporarily suppressed water-column denitrification and interrupted the accumulation of biologically produced excess N_2. The influence of the inflow gradually weakened over subsequent years, after which oxygen depletion and N-loss processes resumed (Myllykangas et al., 2017). Restricting the analysis to 2016–2023 period therefore provides a more robust basis for assessing deep-water ΔN_2 accumulation and net fixed N loss under hydrographic conditions representative of typical stagnation phases in the Baltic Proper.

2.3 Calculation of excess dinitrogen (ΔN_2)

Biologically produced ΔN_2 was derived from the measured N_2/Ar ($(N_2/Ar)_{mes}$) ratio and the expected equilibrium N_2/Ar ($(N_2/Ar)_{sat}$) ratio in seawater (Figure 1). Excess N_2 was calculated according to:

$$\Delta N_2 = \left(\left(\frac{N_2}{Ar} \right)_{mes} - \left(\frac{N_2}{Ar} \right)_{sat} \right) \times Ar_{mes} \quad (1)$$

where Ar_{mes} is the measured dissolved argon concentration in the sample. Because argon is biologically inert and its concentration is controlled primarily by physical processes such as temperature-dependent solubility, salinity, mixing, and air–sea gas exchange, it serves as an internal physical reference tracer. Multiplication by Ar_{mes} converts deviations of the measured N_2/Ar ratio from equilibrium into concentration units of excess dissolved N_2 while normalizing for sample-specific physical effects influencing total dissolved gas concentrations. Positive ΔN_2 values indicate dissolved N_2 in excess of the calculated atmospheric-equilibrium reference. In subhalocline waters during stagnation, the temporal increase in ΔN_2 is interpreted primarily as accumulation of biologically produced N_2, while residual effects of mixing and transport cannot be fully excluded. The equilibrium N_2/Ar ratio was calculated from in situ temperature and salinity assuming solubility equilibrium with the atmosphere, following established formulations summarized in Sivasamy et al. (2025) and references therein, with solubility coefficients from Hamme and Emerson (2004). This atmospheric-equilibrium state represents the reference condition established when water masses were last ventilated at the sea surface. Because subhalocline waters are effectively isolated from direct atmospheric gas exchange after ventilation, positive deviations from this baseline were interpreted as subsequent in situ accumulation of biologically produced N_2. Hydrostatic pressure correction was not applied because the calculation was referenced to atmospheric equilibrium during ventilation rather than hypothetical equilibrium at sampling depth. Hydrostatic pressure effects, therefore, are not explicitly included in the equilibrium solubility calculations based on Hamme and Emerson (2004). While this may contribute to uncertainty in absolute ΔN_2 values in deeper waters, it is not expected to substantially affect the observed spatial patterns or the interpretation of ΔN_2 accumulation as an integrated signal of net N loss.

For model-derived calculations, dissolved Ar concentrations were not available from the ERGOM–MOM output and were therefore approximated by equilibrium Ar concentrations calculated from modeled temperature and salinity. Under this approximation, model-derived ΔN_2 effectively represents the deviation of modeled dissolved N_2 from equilibrium N_2 expected for the corresponding temperature and salinity. This simplification introduces additional uncertainty compared to the observational calculation, where measured Ar explicitly normalizes for sample-specific physical variability. However, because Ar behaves quasi-conservatively in stratified deep waters and is governed primarily by physical processes such as temperature-dependent solubility, mixing, and air–sea exchange (Hamme and Emerson, 2004, 2013), deviations from equilibrium are expected to remain relatively small under stable hydrographic conditions below the permanent halocline. In the stratified deep waters of the Baltic Proper, below the permanent halocline, deviations between measured and equilibrium Ar concentrations are expected to remain relatively small under stable hydrographic conditions. Nevertheless, some uncertainty in model derived ΔN_2 values may arise if physical disequilibrium in Ar occurs due to mixing, temperature variability, or pressure effects. Excess N_2 was interpreted as an integrated signal of net biogeochemical N transformations in the water column and sediment–water exchange fluxes.

In Press

2.4 Estimation of net fixed nitrogen loss from deep-water ΔN_2 accumulation

The analysis focused on water masses located below the permanent halocline, where vertical ventilation is strongly restricted and processes responsible for the removal of fixed N are intensified. During the post-2014 stagnation period, the influence of the major Baltic inflow gradually diminished, leading to substantially reduced vertical ventilation below the halocline. These conditions promoted the progressive accumulation of biologically produced excess N_2 in subhalocline waters. The slope (a) of the linear regression between ΔN_2 and time (year) was interpreted as the rate of ΔN_2 accumulation (Table 2). Differences between observational and model-derived temporal trends were assessed separately for each basin using analysis of covariance (ANCOVA), with ΔN_2 as the response variable, year as a continuous predictor, and source (observation vs. model) as a categorical factor. To ensure direct comparability, these analyses were restricted to subsets of the model output corresponding only to years for which observational data were available within each basin. The significance of the year × source interaction was used to test for differences in temporal trend slopes. To express the results as area-normalized, the estimated deep-water net N_2 accumulation was multiplied by the corresponding subhalocline water volume and subsequently normalized to the basin area occupied by subhalocline waters (Table 2). Halocline depths were defined based on published studies and regional hydrographic characteristics and were set to 80 m for the EGB (Väli et al., 2013), 60 m for the BB (Carstensen et al., 2014), and 70 m for the GB (Paka et al., 2019). These volumes were calculated using GEBCO bathymetry (GEBCO Compilation Group, 2023) and HELCOM subbasin boundaries (HELCOM Secretariat, 2022) processed in R with the packages terra (Hijmans, 2024) and sf (Pebesma, 2018). Under the stagnation conditions considered here, the deep-water ΔN_2 accumulation was converted to N units to obtain a first-order estimate of net fixed N loss according to:

$$D = 2 \times a \times \frac{V}{A} \quad (2)$$

where a is the slope of ΔN_2 accumulation over time, V is the subhalocline water volume, and A is the area occupied by subhalocline waters. The factor of 2 converts molecular N_2 to units of N atoms. Relative standard errors were calculated from the standard error of the regression slope. The resulting estimate is interpreted as the temporal accumulation of excess N_2, rather than as a direct measurement of an instantaneous N-loss process rate (Table 2).

3. Results

3.1 Hydrographic characteristics of the investigated basins

Both model simulations and in situ observations showed clear vertical hydrographic stratification across all three investigated basins, characterized by distinct halocline structures and progressive oxygen depletion below the halocline (Figure 3). In the EGB, both datasets indicated strong stratification, with a pronounced halocline at approximately 60–80 m and a rapid decline in O_2 toward near-anoxic conditions in the deepest layers. This basin exhibited the strongest and most persistent oxygen depletion among the investigated regions.

The BB showed a comparatively shallower water column and weaker vertical stratification, with a less pronounced halocline and substantial O_2 depletion below the halocline.

The GB displayed intermediate hydrographic characteristics, with a distinct halocline and a progressive decline in O_2 toward low-O_2 conditions at depth. While oxygen

Table 2. Linear regression parameters between ΔN_2 and time, halocline depth, subhalocline area and volume, and derived areal net fixed nitrogen loss for the model results and the investigated basins. Relative standard errors were calculated from the standard error of the regression slope.

Area	Halocline depth	Subhalocline area	Water volume	Method	Linear regression	Relative standard error	Net fixed nitrogen loss ±SE	
	[m]	[km^2]	[km^3]			[%]	[mmol N m^{-2} yr^{-1}]	[kt N yr^{-1}]
EGB	80[1]	31959.2	1319.5	Measurements	$y = 2.186a - 4400.0$	28.1	180.5 ± 50.7	80.8 ± 22.7
				Model subset	$y = 0.872a - 1739.6$	4.9	72.0 ± 3.6	32.2 ± 1.6
				Model	$y = 0.733a - 1459.3$	2.6	60.3 ± 1.6	27.0 ± 0.7
BB	60[2]	2172.3	165.1	Measurements	$y = 3.376a - 6804.8$	49.8	95.1 ± 47.4	15.6 ± 7.8
				Model subset	$y = 1.633a - 3286.1$	21.2	46.0 ± 9.8	7.5 ± 1.6
				Model	$y = 0.567a - 1134.0$	15.5	16.0 ± 2.5	2.6 ± 0.4
GB	70[3]	11719.3	43.6	Measurements	$y = 7.632a - 15391.4$	43.9	306.4 ± 134.7	9.3 ± 4.1
				Model subset	$y = 3.562a - 7168.2$	13.0	143.0 ± 18.6	4.3 ± 0.6
				Model	$y = 0.178a - 344.8$	27.1	7.1 ± 1.9	0.2 ± 0.06

[1] Väli et al. (2013)
[2] Carstensen et al. (2014)
[3] Paka et al. (2019)

In Press

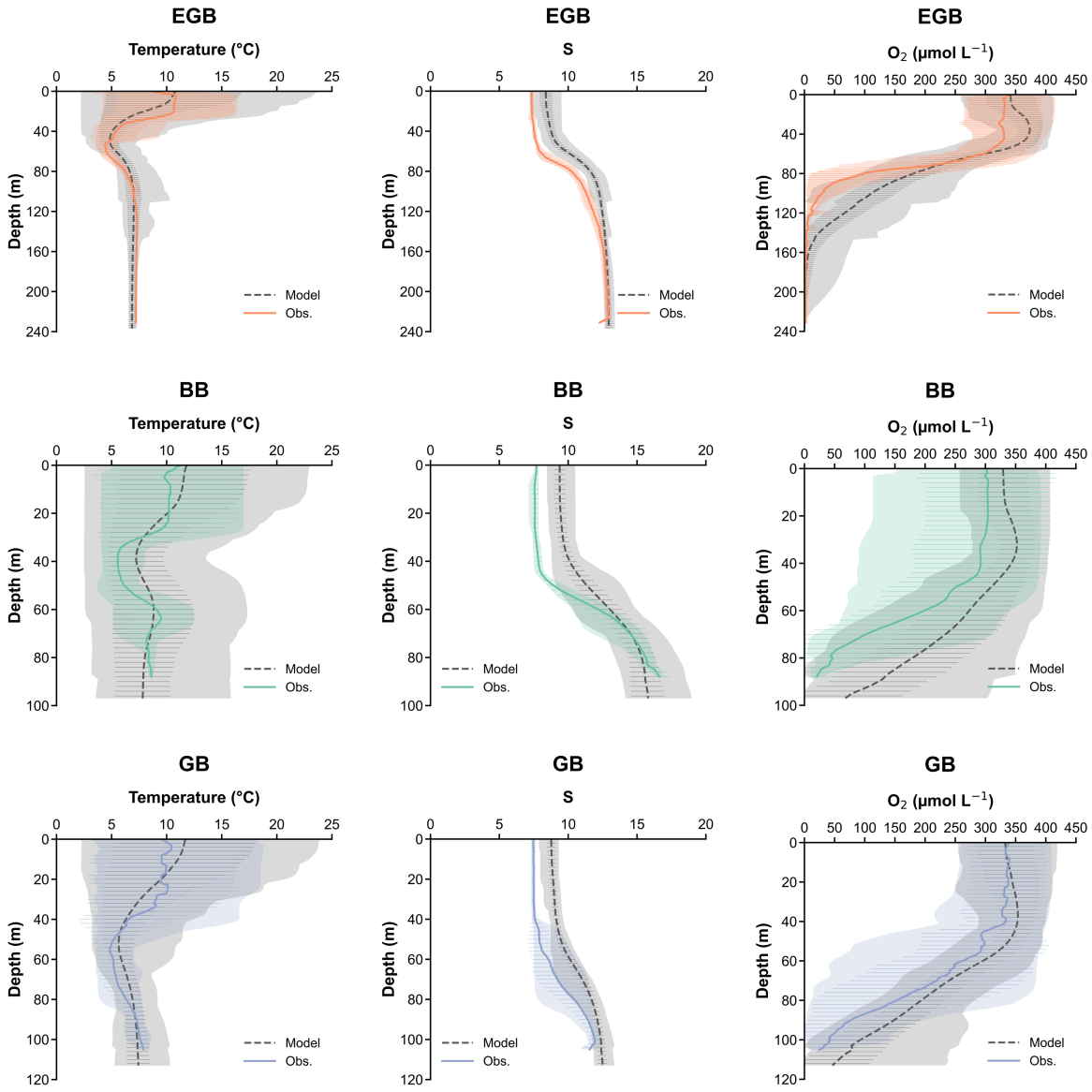


Figure 3. Vertical distributions of temperature (T – left), salinity (S – middle), and dissolved oxygen (O_2 – right) in the Eastern Gotland Basin (EGB), Bornholm Basin (BB), and Gdańsk Basin (GB) derived from in situ observations and model data obtained from the ERGOM–MOM coupled biogeochemical–hydrodynamic model (Neumann et al., 2000, 2022; Diak et al., in press). Solid colored lines represent mean observational profiles, with shaded envelopes indicating observational variability across sampling events. Dashed black lines show corresponding mean modeled profiles, with grey shading indicating model variability over the respective analysis period. In situ T, S, and O_2 measurements were taken from Sivasamy et al. (2025).

depletion was evident in both basins, the most persistent and pronounced deep-water O_2 depletion occurred in the EGB.

Modeled temperature, salinity, and dissolved oxygen profiles reproduced the major hydrographic characteristics observed in all three basins, including basin-specific differences in stratification intensity and deep-water oxygen depletion. The close agreement between modeled and observed vertical hydrographic structure supports the use of the model framework for interpreting basin-scale temporal patterns of ΔN_2 accumulation below the halocline.

3.2 Temporal variability of ΔN_2 below the halocline among Baltic basins

Both in situ observations and model simulations indicated increasing ΔN_2 below the halocline in the Baltic Proper, although the magnitude and temporal variability differed

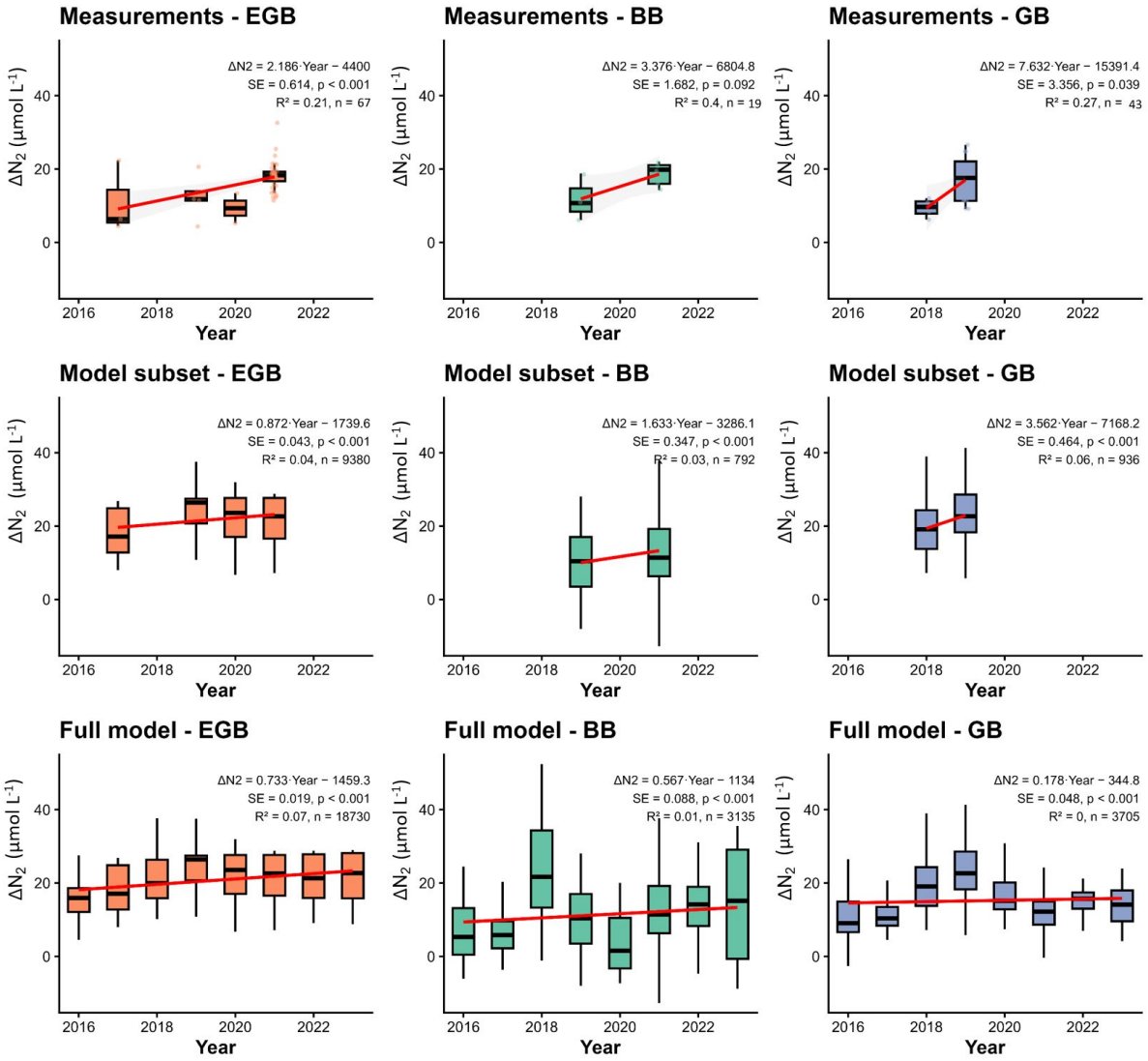


Figure 4. Temporal evolution of excess dinitrogen (ΔN_2) below the halocline in the Eastern Gotland Basin (EGB), Bornholm Basin (BB), and Gdańsk Basin (GB). For each basin, ΔN_2 distributions are shown for in situ observations, temporally matched model subsets extracted for the years corresponding to observational sampling, and the full-model. Model data were obtained from the ERGOM–MOM coupled biogeochemical–hydrodynamic model (Neumann et al., 2000, 2022; Diak et al., in press), while in situ ΔN_2 measurements were taken from Sivasamy et al. (2025). Boxes represent the range (25–75%), thick black lines indicate medians, and whiskers denote minimum–maximum values. Red lines show linear regressions, with statistical parameters reported in each panel. SE denotes the standard error of the regression slope, p indicates statistical significance, R^2 represents the coefficient of determination, and n corresponds to the number of samples.

among basins (Figure 4). In the EGB, measured ΔN_2 values increased significantly between 2017 and 2021, with the regression analysis indicating a strong positive temporal trend despite substantial interannual variability. A similar increasing pattern was observed in the model subset (between 2017 and 2021) extracted for stations corresponding to the measurement locations, as well as in the full-model dataset covering the entire EGB. Although the observational trend was numerically steeper, analysis of covariance (ANCOVA) detected no significant difference between the observational and temporally matched model-subset regressions ($p = 0.105$).

In the BB, measured ΔN_2 values also exhibited an increasing tendency between 2019 and 2021, although the limited number of observations resulted in higher uncertainty, reflected by larger standard errors (SE) and a weaker statistical significance. Nevertheless, both the model subset and the full-model dataset supported the presence

of a positive long-term trend in ΔN_2 accumulation below the halocline. No significant difference was detected between observational and model-subset regressions (ANCOVA, $p = 0.625$).

The strongest temporal increase in measured ΔN_2 was observed in the GB during 2018–2019. This pattern was also reproduced by the model subset, which showed a pronounced positive trend in ΔN_2 accumulation. In contrast, the full-model dataset for the GB indicated only a weak increase over the broader 2016–2023 period, suggesting stronger temporal variability and less persistent basin-wide accumulation compared to the EGB. However, the observational and model-subset regressions were not significantly different (ANCOVA, $p = 0.323$).

The absence of statistically significant differences between observational regressions and temporally matched model-subset regressions indicates that modeled temporal ΔN_2 trends are consistent with observations within observational uncertainty. This agreement supports cautious interpretation of the full-model simulations as representative of basin-scale ΔN_2 accumulation dynamics below the halocline during the stagnation period. Together, these results support the interpretation that excess N_2 progressively accumulated below the halocline during stagnation conditions, consistent with sustained net fixed N loss in the Baltic Proper.

4. Discussion

4.1 Net fixed nitrogen loss

MBIs, such as those recorded in 1993, 2003, and the exceptionally strong event of December 2014, temporarily ventilate deep Baltic basins but do not permanently disrupt stratification. The 2014 MBI introduced approximately 198 km^3 of saline, O_2-rich water and ~4 Gt of salt into the Baltic Sea, ranking among the three strongest inflows since 1880 (Mohrholz et al., 2015). By 2016, the direct influence of the inflow had largely subsided, and the Baltic Proper returned to conditions characterized by progressive O_2 depletion and renewed redox stratification (Myllykangas et al., 2017). Consequently, the present analysis focused on the post-2014 stagnation period, during which reduced vertical ventilation below the halocline allowed biologically produced excess N_2 to progressively accumulate in subhalocline waters. Under such conditions, deep waters below the halocline behave as semi-isolated water masses in which temporal biogeochemical changes can be interpreted as integrated transformation signals over time (Schneider et al., 2010).

The interpretation of ΔN_2 as an estimate on fixed N loss is consistent with previous applications of N_2/Ar measurements. Chang et al. (2012) used excess N_2 to estimate net fixed N loss in oceanic oxygen-deficient zones, while Shigemitsu et al. (2016) demonstrated that ΔN_2/Ar can provide a constraint on fixed-nitrogen removal associated with water-column and benthic denitrification. In contrast to these open-ocean applications, the present study uses the temporal accumulation of ΔN_2 in subhalocline waters during stagnation. The restricted ventilation of these deep-water masses allows changes in ΔN_2 inventory over time to be interpreted as a first-order estimate on net fixed N loss in the Baltic Sea from deep-water excess N_2 accumulation although N_2 consumption through N_2 fixation, physical transport and mixing remain sources of uncertainty.

Net fixed N loss derived from in situ observations amounted to approximately 80.8 kt N yr^{-1} in the EGB, ~15.6 kt N yr^{-1} in the BB, and ~9.3 kt N yr^{-1} in the GB (Table 2). Corresponding estimates derived from temporally matched model subsets extracted for the observational stations were consistently lower, reaching ~32.2 kt N yr^{-1} in the EGB, ~7.5 kt N yr^{-1} in the BB, and ~4.3 kt N yr^{-1} in the GB. Full-model basin-scale simulations yielded even lower values, particularly in the GB (~0.2 kt N yr^{-1}). However, basin-specific ANCOVA comparisons detected no significant differences between observational and temporally matched model-derived ΔN_2 accumulation slopes, indicating that modeled temporal trends were statistically consistent with observations within observational uncertainty. This agreement supports cautious interpretation of the full-model simulations as first-order basin-scale representations of subhalocline ΔN_2 accumulation dynamics during the stagnation period.

Relative standard errors ranged from 3 to 50%, with the highest uncertainties associated with basins characterized by limited observational coverage and stronger hydrographic variability. The comparatively lower values obtained in the present study relative to previous Baltic Sea estimates likely result from methodological and conceptual differences. Schneider et al. (2010) reported denitrification rates up to ~456 kt N yr^{-1} during prolonged stagnation following the 2003 MBI, while Dalsgaard et al. (2013) estimated denitrification in the Baltic Proper to range from 132 to 547 kt N yr^{-1} using incubation and mass-balance approaches. Basin-wide modeling by Gustafsson et al. (2017) suggested total denitrification rates of 1153 ± 60 kt N yr^{-1} for the Eastern Baltic Sea, although only $\sim 105 \pm 54$ kt N yr^{-1} was attributed to water-column denitrification. Unlike incubation-based approaches targeting instantaneous process rates, the N_2/Ar method quantifies accumulated excess N_2 and therefore reflects integrated net changes in dissolved N_2 over time. Consequently, ΔN_2 accumulation reflects the balance between biological N_2 production, and physical transport. Under low-oxygen conditions, part of the produced N_2 may be offset by benthic or suboxic N_2 fixation by non-cyanobacterial diazotrophs documented in Baltic Sea environments (Farnelid et al., 2013; Bentzon-Tilia et al., 2015). Detectable N_2 fixation activity and nifH gene expression have been reported from anoxic Baltic environments (Bertics et al., 2013; Farnelid et al., 2013), although the quantitative importance of this pathway remains uncertain.

In Press

Existing Baltic Sea N budgets remain difficult to constrain because N-loss processes are spatially heterogeneous and strongly influenced by O_2 availability, sulfide concentrations, temperature, sediment characteristics, and NO_3^- supply. Published basin-scale denitrification estimates range widely, from approximately 300 to 1250 kt N yr^{-1} (Deutsch et al., 2010; Gustafsson et al., 2017; Lønborg and Markager, 2021), partly reflecting methodological differences among incubation experiments, mass-balance approaches, and model simulations. The N_2/Ar approach therefore provides a complementary basin-scale indicator of net fixed N loss by integrating the cumulative effects of biological N_2 production via denitrification and anammox, N_2 consumption through N_2 fixation, and physical processes such as mixing and transport occurring below the halocline during stagnation periods.

4.2 Inconsistencies between model-derived and observation-based estimates

Model-derived net fixed N loss reproduced the same temporal trends as the observation-based estimates across all investigated basins, although modeled rates were consistently lower. Basin-specific analysis of covariance (ANCOVA) comparing observational regressions with temporally matched model subsets detected no significant differences in temporal slopes (EGB: $p = 0.105$, BB: $p = 0.625$, GB: $p = 0.323$), indicating that modeled and observational ΔN_2 accumulation trends were statistically comparable within observational uncertainty. Nevertheless, the consistently lower model-derived estimates suggest a systematic tendency toward underestimation.

These discrepancies likely reflect unequal sampling density, unresolved small-scale redox variability, and limitations in the simulated hydrographic structure. In particular, transient low-oxygen microenvironments below the halocline are difficult to resolve in basin-scale models and may contribute to underestimation of biologically produced excess N_2 accumulation.

The combined observational–modeling approach demonstrated that ΔN_2 accumulation below the halocline was not restricted to individual stations but represented a coherent basin-scale feature. Both temporally matched model subsets and full-model basin simulations reproduced positive ΔN_2 trends below the halocline (Figure 4; Table 2), supporting cautious interpretation of the full-model results as representative of basin-scale subhalocline dynamics.

The strongest and most coherent accumulation occurred in the EGB, where persistent O_2 depletion and prolonged stagnation favor N-loss processes in deep waters. In contrast, the BB and GB exhibited greater temporal variability and higher uncertainty, reflecting more dynamic hydrographic conditions and reduced observational coverage. The Bornholm Basin is particularly influenced by episodic inflows through the Danish Straits, which rapidly modify stratification and redox conditions, complicating both observational interpretation and model representation. The comparatively low full-model estimates in the GB may additionally reflect strong spatial heterogeneity associated with riverine influence and episodic ventilation (Kuliński et al., 2022), processes that are difficult to fully resolve using limited station-based observations.

4.3 Uncertainty

Uncertainty in the calculated deep-water ΔN_2 accumulation and consequently, net fixed N loss arises from several methodological, analytical, and environmental factors associated with both ΔN_2 determination and extrapolation from local observations to basin scales.

The primary source of uncertainty is related to the linear regression used to estimate temporal ΔN_2 accumulation rates. This uncertainty is expressed as the standard error of the regression slope (Table 2; Figure 4). Relative standard errors of the calculated deep-water ΔN_2 accumulation ranged from 3 to 50%. The measurement-based approach was particularly affected by the limited number of in situ observations, whereas the model-derived ΔN_2 calculations additionally depended on modeled hydrographic conditions, including temperature and salinity, which introduces an additional source of uncertainty.

Additional uncertainty originates from the analytical precision of the N_2/Ar measurements ($\pm 0.05\%$ for N_2/Ar ratios) and assumptions regarding equilibrium Ar concentrations. Because dissolved Ar concentrations were not available from the model output, Ar concentrations in the model calculations were approximated by equilibrium values derived from modeled temperature and salinity. This simplification effectively reduces the explicit inert-gas normalization applied in the observational calculations and introduces uncertainty where physical Ar disequilibrium occurs below the halocline. Although this assumption is supported by the quasi-conservative behavior of Ar in deep stratified waters, deviations caused by mixing or residual ventilation may introduce an uncertainty into calculated ΔN_2 values, estimated to be on the order of ~5%.

Further uncertainty is associated with the definition of halocline depth and the resulting estimates of subhalocline water volumes and basin areas used for extrapolation. Because these depth thresholds were adopted from published literature, some over- or underestimation of the effective subhalocline volume cannot be excluded.

An additional source of uncertainty is related to physical transport and mixing processes. Although the post-2014 stagnation period was characterized by strongly reduced deep-water ventilation, the Baltic Proper cannot be considered a perfectly closed system. Consequently, ΔN_2 accumulation below the halocline reflects the integrated balance between biological N_2 production, potential N_2 fixation, vertical mixing, and lateral transport rather than direct instantaneous denitrification alone.

In Press

5. Conclusions and recommendations

The post-2014 inflow period analyzed here represented a hydrographic regime characterized by renewed stratification and O_2 depletion below the halocline, conditions that favored accumulation of biologically produced N_2 in deep waters. The consistent increase in ΔN_2 observed in both model results and in situ data indicated deep-water ΔN_2 accumulation during stagnation phases. Basin-scale rates derived from ΔN_2 trends varied among regions, reflecting differences in hydrography, basin geometry, and data coverage.

The strongest and most persistent ΔN_2 accumulation was observed in the Eastern Gotland Basin, whereas the Bornholm and Gdańsk basins exhibited greater variability and uncertainty associated with more dynamic hydrographic conditions and reduced observational coverage. First-order estimates of net fixed N loss derived from ΔN_2 accumulation amounted to approximately 80.8 ± 22.7 kt N yr^{-1} in the EGB, $\sim 15.6 \pm 7.8$ kt N yr^{-1} in the Bornholm Basin (BB), and $\sim 9.3 \pm 4.1$ kt N yr^{-1} in the Gdańsk Basin (GB), although estimates for the BB and GB should primarily be interpreted as preliminary first-order basin-scale estimates constrained by limited observational coverage.

The obtained values fall within the lower range of previously published Baltic Sea N-loss estimates. Because dissolved excess N_2 is derived from N_2/Ar measurements, the resulting signal integrates cumulative contributions from both pelagic and benthic N-loss and gain processes while also reflecting transport and mixing. Because ΔN_2 integrates the cumulative effects of multiple biological and physical processes occurring below the halocline, repeated N_2/Ar observations, which are comparatively simple, cost-effective, and integrative over time, may provide a practical indicator of temporal changes in deep-water N cycling that complements process-specific measurements and ecosystem models.

Acknowledgements

This study was supported by the statutory activities of the Institute of Oceanology of the Polish Academy of Sciences (IO PAN), task II.9, and by the National Science Centre (NCN, Poland) under projects no. 2021/05/X/ST6/00898 and 2019/34/E/ST10/00217. We thank Pratha Sivasamy, Piotr Prusiński, Przemysław Makuch, Aleksandra Winogradow, Marta Borecka, Karol Kuliński and Katarzyna Koziorowska for their support with data collection and analysis. We also acknowledge Thomas Neumann and Markus Meier for providing access to and support with the ERGOM–MOM model framework, and Hermann W. Bange for valuable scientific discussions.

Data availability

In situ data are available here: https://doi.org/10.48457/iopan-2024-253. Model data can be extracted from ERGOM-MOM 5.1.

Conflict of interest

None declared.

References

Bentzon-Tilia, M., Severin, I., Hansen, L.H., Riemann, L., 2015. *Genomics and Ecophysiology of Heterotrophic Nitrogen-Fixing Bacteria Isolated from Estuarine Surface*. Water. MBio 6, e00929. https://doi.org/10.1128/mBio.00929-15

Bertics, V.J., Löscher, C.R., Salonen, I., Dale, A.W., Gier, J., Schmitz, R.A., Treude, T., 2013. *Occurrence of benthic microbial nitrogen fixation coupled to sulfate reduction in the seasonally hypoxic Eckernförde Bay, Baltic Sea*. Biogeosciences 10, 1243–1258, https://doi.org/10.5194/bg-10-1243-2013

Bonaglia, S., Klawonn, I., De Brabandere, L., Deutsch, B., Thamdrup, B., Brüchert, V., 2016. *Denitrification and DNRA at the Baltic Sea oxic–anoxic interface: Substrate spectrum and kinetics*. Limnol. Oceanogr. 615, 1900–1915. https://doi.org/10.1002/lno.10343

Capone, D.G., Bronk, D.A., Mulholland, M.R., Carpenter, E.J., 2008. *Nitrogen in the Marine Environment*, Acad. Press, San Diego. https://doi.org/10.1016/B978-0-12-372522-6.X0001-1

Carstensen, J., Andersen, J.H., Gustafsson, B.G., Conley, D.J., 2014. *Deoxygenation of the Baltic Sea during the last century*. Proc. Natl. Acad. Sci. USA, 11115., 5628–5633. https://doi.org/10.1073/pnas.1323156111

Chang, B.X., Devol, A.H., Emerson, S.R., 2012. *N_2 production in oxygen minimum zones*. Deep-Sea Res. Pt. I 65, 131–145. https://doi.org/10.1016/j.dsr1.2012.03.004

Codispoti, L.A., Brandes, J.A., Christensen, J.P., Devol, A.H., Naqvi, S.W.A., Paerl, H.W., Yoshinari, T., 2001. *The oceanic fixed nitrogen and nitrous oxide budgets: Moving targets as we enter the Anthropocene?* Sci. Mar. 65S2, 85–105. https://doi.org/10.3989/scimar.2001.65s285

Dalsgaard, T., De Brabandere, L., Hall, P.O., 2013. *Denitrification in the water column of the central Baltic Sea*. Geochim. Cosmochim. Acta 106, 247–260. https://doi.org/10.1016/j.gca.2012.12.038

Deutsch, B., Forster, S., Wilhelm, M., Dippner, J.W., Voss, M., 2010. *Denitrification in sediments as a major nitrogen sink in the Baltic Sea: an extrapolation using sediment characteristics*. Biogeosciences 7 (10), 3259–3271. https://doi.org/10.5194/bg-7-3259-2010

Devol, A., Uhlenhopp, A., Naqvi, S., Brandes, J., Jayakumar, D., Naik, H., Gaurin, S., Codispoti, L., Yoshinari, T., 2006. *Denitrification rates and excess nitrogen gas concentrations in the Arabian Sea oxygen deficient zone*. Deep-

In Press

Sea Res. Pt. I, 539, 1533–1547. https://doi.org/10.1016/j.dsr.2006.07.005

DeVries, T., Deutsch, C., Primeau, F., Chang, B., Devol, A., 2012. *Global rates of water-column denitrification derived from nitrogen gas measurements*. Nat. Geosci. 58., 547–550. https://doi.org/10.1038/ngeo1515

Diak, M., Kuliński, K., Meier, H.E.M., Neumann, T., Winogradow, A., Szymczycha, B., 2026, *Integration of model and observational data of excess dinitrogen gas below the halocline in the Baltic Sea*. Oceanologia, in press.

Farnelid, H., Bentzon-Tilia, M., Andersson, A.F., Bertilsson, S., Jost, G., Labrenz, M., Jürgens, K., Riemann, L., 2013. *Active nitrogen-fixing heterotrophic bacteria at and below the chemocline of the central Baltic Sea*. ISME J. 77, 1413–1423. https://doi.org/10.1038/ismej.2013.26

GEBCO Compilation Group, 2023. *GEBCO_2023 Grid* [bathymetric dataset]. https://www.gebco.net/data_products/gridded_bathymetry_data/; https://doi.org/10.5285/f98b053b-0cbc-6c23-e053-6c86abc0af7b

Grabski, M., Kotlarska, E., Łuczkiewicz, A., Hryniewicz, K., Węgrzyn, G., Szymczycha, B., 2025. *Spatial and seasonal distribution of selected nitrogen cycle genes in deep waters of the Baltic Proper*. Front. Mar. Sci. 12, 1456825. https://doi.org/10.3389/fmars.2025.1456825

Gräwe, U., Naumann, M., Mohrholz, V., Burchard, H., 2015. *Anatomizing one of the largest saltwater inflows into the Baltic Sea in December 2014*. Geophys. Res. Oceans 120, 7676–7697. https://doi.org/10.1002/2015JC011269

Groffman, P.M., Altabet, M.A., Böhlke, H., Butterbach-Bahl, K., David, M.B., Firestone, M.K., Giblin, A.E., Kana, T.M., Nielsen, L.P., Voytek, M.A., 2006. *Methods for measuring denitrification: diverse approaches to a difficult problem*. Ecol. Appl. 16 (6), 2091–2122. https://doi.org/10.1890/1051-0761(2006)016[2091:mfmdda]2.0.co;2

Gustafsson, E., Savchuk, O.P., Gustafsson, B.G., Müller-Karulis, B., 2017. *Key processes in the coupled carbon, nitrogen, and phosphorus cycling of the Baltic Sea*. Biogeochemistry 134, 301–317. https://doi.org/10.1007/s10533-017-0361-6

Hamme, R.C., Emerson, S.R., 2004. *The solubility of neon, nitrogen and argon in distilled water and seawater*. Deep-Sea Res. Pt. I, 5111, 1517–1528. https://doi.org/10.1016/j.dsr.2004.06.009

Hamme, R.C., Emerson, S.R., 2013. *The role of dissolved gases in marine biogeochemistry*. Annu. Rev. Mar. Sci. 5, 33–60. https://doi.org/10.1073/pnas.2217946120

Hamme, R.C., Severinghaus, J.P., 2007. *Trace gas solubility in seawater*. Geophys. Res. Lett. 34, L19608.

HELCOM Secretariat., 2022. *HELCOM subbasins with coastal and offshore division 2022 level 3* [Dataset]. HELCOM Metadata catalogue. https://metadata.helcom.fi/geonetwork/srv/api/records/e5a59af9-c244-4069-9752-be3acc5dabed

Hietanen, S., Kuparinen, J., 2008. *Seasonal and short-term variation in denitrification and anammox at a coastal station on the Gulf of Finland, Baltic Sea*. Hydrobiologia, 5961, 67–77. https://doi.org/10.1007/s10750-007-9058-5

Hijmans, R.J., 2024. *Spatial data analysis R package*. https://CRAN.R-project.org/package=terra

Kuliński, K., Rehder, G., Asmala, E., Bartosova, A., Carstensen, J., Gustafsson, B., Hall, P.O.J., Humborg, C., Jilbert, T., Jürgens, K., Meier, H.E.M., Müller-Karulis, B., Naumann, M., Olesen, J.E., Savchuk, O., Schramm, A., Slomp, C.P., Sofiev, M., Sobek, A., Szymczycha, B., Undeman, E., 2022. *Biogeochemical functioning of the Baltic Sea*. Earth Syst. Dynam. 131, 633–685. https://doi.org/10.5194/esd-13-633-2022

Lam, P., Kuypers, M.M.M., 2011. *Microbial nitrogen cycling processes in oxygen minimum zones*. Annu. Rev. Mar. Sci. 3, 317–345. https://10.1146/annurev-marine-120709-142814

Loeffler, A., Schneider, B., Schmidt, M., Nausch, G., 2011. *Estimation of denitrification in Baltic Sea deep water from gas tension measurements*. Mar. Chem. 1251-4, 91–100.

Lønborg, C., Markager, S., 2021. *Nitrogen in the Baltic Sea: Long-term trends, a budget and decadal time lags in responses to declining inputs*. Estuar. Coast. Shelf Sci. 261, 107529. https://doi.org/10.1016/j.ecss.2021.107529

Mazur-Marzec, H., Andersson, A.F., Błaszczyk, A., Dąbek, P., Górecka, E., Grabski, M., Jankowska, K., Jurczak-Kurek, A., Kaczorowska, A.K., Kaczorowski, T., Karlson, B., Kataržytė, M., Kobos, J., Kotlarska, E., Krawczyk, B., Łuczkiewicz, A., Piwosz, K., Rybak, B., Rychert, K., Sjöqvist, C., Surosz, W., Szymczycha, B., Toruńska-Sitarz, A., Węgrzyn, G., Witkowski, A., Węgrzyn, A., 2024. *Biodiversity of microorganisms in the Baltic Sea: the power of novel methods in the identification of marine microbes*. FEMS Microbiol. Rev. 485. https://doi.org/10.1093/femsre/fuae024

Meier, H.E.M., 2007. *Modeling the pathways and ages of inflowing salt-and freshwater in the Baltic Sea*. Estuar. Coast. Shelf Sci. 74, 610–627. https://doi.org/10.1016/j.ecss.2007.05.019

Meyer, R.L., Allen, D.E., Schmidt, S., 2008. *Nitrification and denitrification as sources of sediment nitrous oxide production: A microsensor approach*. Mar. Chem. 110 (1), 68–76. https://doi.org/10.1016/j.marchem.2008.02.004

In Press

Mohrholz, V., 2018. *Major Baltic inflow statistics – revised*. Front. Mar. Sci. 5, 384. https://doi.org/10.3389/fmars.2018.00384

Mohrholz, V., Naumann, M., Nausch, G., Krüger, S., Gräwe, U., 2015. *Fresh oxygen for the Baltic Sea – An exceptional saline inflow after a decade of stagnation*. J. Mar. Syst. 148, 152–166. https://doi.org/10.1016/j.jmarsys.2015.03.005

Myllykangas, J.P., Jilbert, T., Jakobs, G., Rehder, G., Werner, J., Hietanen, S., 2017. *Effects of the 2014 major Baltic inflow on methane and nitrous oxide dynamics in the water column of the central Baltic Sea*. Earth Syst. Dyn. 8, 817–826. https://doi.org/10.5194/esd-8-817-2017

Neumann, T., 2000. *Towards a 3D-ecosystem model of the Baltic Sea*. J. Mar. Syst. 253-4, 405–419. https://doi.org/10.1016/S0924-7963(00)00030-0

Neumann, T., Radtke, H., Cahill, B., Schmidt, M., 2022. *Non-Redfield carbon model for the Baltic Sea ERGOM version 1.2. – Implementation and Budget estimates*. Geosci. Model Dev. Discuss, 1–131. https://doi.org/10.5194/gmd-15-8473-2022

Nielsen, L.P., Glud, R.N., 1996. *Denitrification in a coastal sediment measured in situ by the nitrogen isotope pairing technique applied to a benthic flux chamber*. Mar. Ecol. Prog. Ser, 137, 181–186.

Paka, V.T., Zhurbas, V.M., Golenko, M.N., Korzh, A.O., Kondrashov, A.A., Shchuka, S.A., 2019. *Innovative closely spaced profiling and current velocity measurements in the Southern Baltic Sea in 2016–2018 with special reference to the bottom layer*. Front. Earth Sci. 7, 111. https://doi.org/10.3389/feart.2019.00111

Pebesma, E., 2018. *Simple Features for R*. The R Journal 101, 439–446. https://doi.org/10.32614/RJ-2018-009

Risgaard-Petersen, N., Nielsen, L.P., Rysgaard, S., Dalsgaard, T., Meyer, R.L., 2003. *Application of the isotope pairing technique in sediments where anammox and denitrification coexist*. Limnol. Oceanogr. Methods, 1. https://doi.org/10.4319/lom.2003.1.63.

Schneider, B., Nausch, G., Pohl, C., 2010. *Mineralization of organic matter and nitrogen transformations in the Gotland Sea deep water*. Mar. Chem. 1191-4. 153–161. https:doi.org/10.1016/j.marchem.2010.02.004

Shigemitsu, M., Gruber, N., Oka, A., Yamanaka, Y., 2016. *Potential use of the N_2/Ar ratio as a constraint on the oceanic fixed nitrogen loss*. Glob. Biogeochem. Cy. 30. https://doi.org/10.1002/2015GB005297

Sivasamy, P., Diak, M., Winogradow, A., Bange, H.W., Borecka, M., Makuch, P., Koziorowska-Makuch, K., Kuliński, K., Mackiewicz, A., Szymczycha, B., 2025. *Spatial and seasonal variability of excess dinitrogen gas in the Baltic Sea*. Front. Mar. Sci. 12, 1455803. https://doi.org/10.3389/fmars.2025.1455803

Szymczycha, B., Zaborska, A., Bełdowski, J., Kuliński, K., Beszczyńska-Möller, A., Kędra, M., Pempkowiak, J., 2019. *World Seas: An Environmental Evaluation*, Acad. Press, 85–111.

Väli, G., Meier, H.M., Elken, J., 2013. *Simulated halocline variability in the Baltic Sea and its impact on hypoxia during 1961–2007*. J. Geophys. Res. Oceans 11812, 6982–7000. https://doi.org/10.1002/2013JC009192

in press